The Influence of Porosity on the Elasticity and Strength of Alumina and Zirconia Ceramics

Nickolai Savchenko[1, a)], Irina Sevostyanova[1, b)], Tatiana Sablina[1, c)], László Gömze[2, d)], and Sergei Kulkov[3, 4, e)]

[1] *Institute of Strength Physics and Materials Science SB RAS, Tomsk, 634055, Russia*
[2] *University of Miskolc, Miskolc-Egyetemvros, H-3515, Hungary*
[3] *National Research Tomsk State University, Tomsk, 634050, Russia*
[4] *National Research Tomsk Polytechnic University, Tomsk, 634050, Russia*

[a)] Corresponding author: savnick@ispms.tsc.ru
[b)] sevir@ispms.tsc.ru
[c)] sabtat@ispms.tsc.ru
[d)] femgömze@uni-miskolc.hu
[e)] kulkov@ms.tsc.ru

Abstract. This work investigates the behavior of porous alumina (with the porosity ranging from 18% to 70%) and zirconia (with the porosity ranging from 10% to 60%) ceramics when subjected to deformation by compression and shearing. The analysis of stress-strain curves showed that there is a transition from a typical brittle state for relatively dense ceramics, to a pseudo-plastic one for ceramics with high porosity. The values of the effective Young's modulus, effective shear modulus and Poisson's ratio decrease with the increase of the pore space volume of ceramics, which correlates with the appearance of multiple cracking during the deformation of the high porosity ceramics.

Keywords: Al_2O_3, ZrO_2, mechanical properties, porous material, Poisson's ratio, strength

INTRODUCTION

It is known that the porosity of brittle materials can have a significant influence on their physical properties (mechanical, thermal, electrical). Young's modulus, shear modulus and Poisson's ratio are essential parameters in the study of advanced material mechanics [1–3]. In addition, the macroscopic behavior of ceramics can vary from brittle to quasi-plastic depending on the pore space volume [4, 5]. That is why investigating the evolution of deformation in a brittle porous material at different scale levels and the subsequent occurrence of failures depending on the deformation rate, constraints, etc. is of considerable interest in terms of the emergence of a structural hierarchy of deformation and destruction in similar brittle materials (ceramics, geological materials).

The objective of the work is to study the relations between parameters such as porosity, compressive strength, effective Young's modulus and effective shear modulus measured during the mechanical loading under compression and shearing, as well as structure of failures and deformations in alumina and zirconia ceramics.

EXPERIMENTAL MATERIALS AND METHODS

Alumina and zirconia ceramics with different porosity levels (10%–70%) were made of Al_2O_3 и ZrO_2–3 wt.% MgO powders obtained by the thermal decomposition of aqueous nitric-acid metallic salt solutions in high-frequency discharge plasma [6]. Initial powders and a 3% solution of polyvinyl in ethyl alcohol were compressed in steel die molds using a hydraulic press with the pressure of 1 t/cm^2 in order to obtain cylindrical (10 mm in diameter,

International Conference on Physical Mesomechanics of Multilevel Systems 2014
AIP Conf. Proc. 1623, 547-550 (2014); doi: 10.1063/1.4899003

15 mm in height) and cubic (10 mm each side) samples. Sintering was performed in air at the temperature ranging from 1000°C to 1650°C with isothermal exposure for one hour. The density of the sintered specimens was measured using the geometrical method. Residual porosity was calculated from the ratio of theoretical density to a measured density, considering the phase composition of the obtained materials. The structure of specimens after sintering was studied using the optical metallography method. The specimens were exposed to mechanical tests for compression and shearing using Instron 1185 universal testing machine with simultaneous recording of a loading diagram. The traversal (loading) rate was 0.2 mm/min. On σ–ε deformational curves, a straight-line segment was outlined, which corresponds to elastic deformation. Effective Young's modulus (*E*) and shearing modulus (*G*) were defined as the angle of a tangent line slope to a straight-line segment of the σ–ε curve.

EXPERIMENTAL RESULTS AND THEIR DISCUSSION

The comparison of σ–ε diagrams, obtained after testing ceramics with different porosity levels at compression, showed that their behavior depends on the pore space volume. The deformation curve analysis of 20% porous Al_2O_3 ceramics proved that they retain linearity of σ–ε functions up to the material fracture (Fig. 1, curve *1*), while the deviations from the linearity are observed in ceramics with a higher porosity ranging from 20% to 70% in the area of high stresses (Fig. 1, curves *2*, *3*).

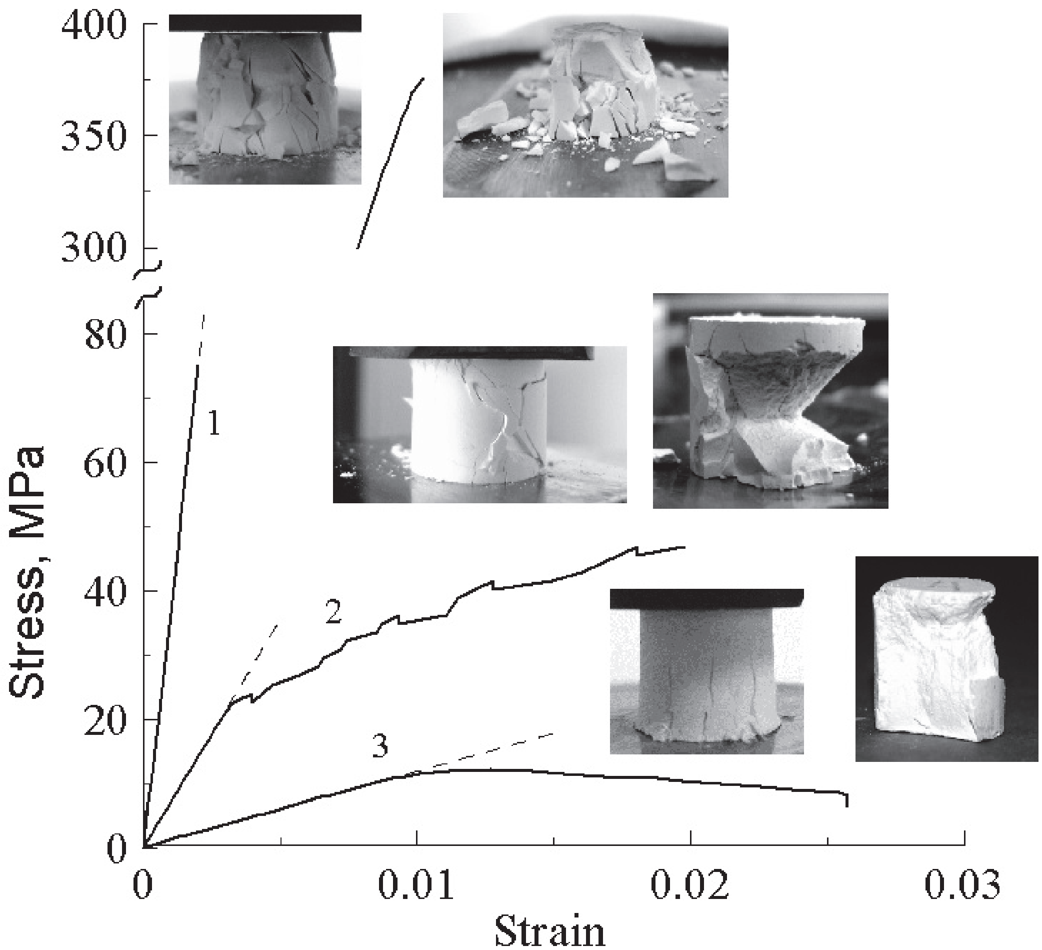

FIGURE 1. "Strain–stress" diagrams and state of specimens obtained after compression tests of Al_2O_3 with porosity of 20% (*1*), 50% (*2*) and 65% (*3*)

The “strain-stress” diagrams of ZrO_2–MgO ceramics obtained after compression and shearing tests of samples with different level of porosity were similar to those shown in Fig. 1 for alumina. The difference in the deformation behavior between ZrO_2–MgO and Al_2O_3 is that the transition from the typically brittle state to a pseudo-plastic one occurred at the lower level of porosity.

Observations of the structure of specimens after compression tests identified some differences in the nature of damage of ceramics with different porosity. In Al_2O_3 specimens with 18%–20% porosity, the brittle fracturing of elastic specimens occurred after the elastic energy accumulation. Due to the elastic energy release, the specimen fully breaks down after reaching the compression strength limit (Fig. 1). With the growth of pore space volume the failures of ceramics became more localized, which lead to partial destruction of specimens after reaching the compression strength limit, while they did not lose the capability of further deformation. The specimens with the porosity of about 50% subjected to compression tests are shown in Fig. 1. It is clear that on the lateral surface of cylindrical specimens, cracks formed at the angle of 45° to the axis of applied load. In such ceramics, the damage zone after compression forms a truncated cone with the cone angle of about 45°, while the cone base lies almost in the plane with the fixed platen of the machine. The deformation of ceramics with the porosity ranging from 50% to 70% is accompanied by the appearance of multiple cracks primarily directed in parallel to the loading axis on the lateral surface of the cylindrical specimen (Fig. 1). Moreover, the base diameter of the cone forming in the fractured specimen was relatively smaller as compared to the denser ceramics, while the taper angle of the cone was approximately 45°. During the shearing tests, Al_2O_3 specimens with the porosity ≤40 % demonstrated the formation of a main crack which was inclined at 45° to the axis of applied load. The main crack appeared at the deformation stage right after the elastic section on the “strain-stress” curve. In specimens with the porosity exceeding 40%, the deformation process was accompanied by the appearance of large number of fine cracks in various directions without obvious main crack up to the stage of complete destruction.

In spite of the general similarity of fracture zones in both Al_2O_3 and ZrO_2–MgO ceramics after compression tests and shear, the ZrO_2–MgO samples with the porosity of 11% form a truncated cone-shaped fracture zone with the angle of 30°.

It is known that cracks appear at the strain localization zones in the most damaged areas of the material [5]. In the case when strain is formed at some angle to the compression axis, the stress related to the presence of friction between the platen of the testing machine and adjacent ends of the sample plays a significant role in the fracturing [7]. Accordingly, the formation of cones inside of the collapsed samples (Fig. 1) due to the presence of friction forces and the destruction of ceramics under compression is controlled by shearing stresses.

It is also known that the orientation of cracks depends on the accumulated strain limit value, or dilatancy (micro-crack saturation and their opening) [5]. Each pore is a potential source of microcracking in a porous material, and with the increase of the number of pores in a specimen the number of such sources naturally grows. Thus, the visible distinctions in the direction and behavior of crack propagated in ceramics with the different level of porosity (Fig. 2) are, apparently, the result of different levels and nature of deformations accumulated in the form of microcracks that appear after compression and shearing.

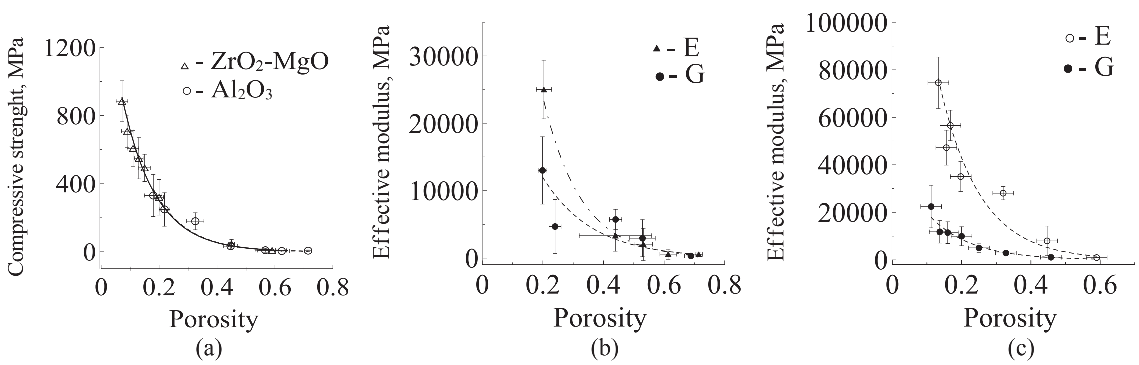

FIGURE 2. Dependence of (a) compressive strength and (c, d) effective Young’s modulus and effective shear modulus values on pore space volume of (a, b) alumina and (a, c) zirconia ceramics

Studies of the mechanical and elastic properties of alumina and zirconia ceramics showed that within the studied intervals of pore space volume, the strength limit under compression, as well as the elasticity and shearing moduli decrease with the increase of porosity (Fig. 2). In addition, the dependency of changes in strength properties on porosity is well-described by the law close to exponential one. As seen in Fig. 2b and 2c, the absolute values of the effective elasticity and effective shearing modulus grow closer with the increase of porosity, which shows a decrease in Poisson's ratio. It should be noted that in our case there is only a decrease in Poisson's ratio values. Determining the absolute values of Poisson's ratio in the process of mechanical testing was complicated since the experimental error was ±0.3. The identification of Poisson's ratio by measuring the rate of longitudinal and latitudinal sound waves [1] in the ceramics performed with the use of an ultrasound flaw detector showed that values of Poisson's ratio decreased from 0.21 to 0.15 with a growth in pore space volume from 20% to 40% in alumina ceramic, while values of Poisson's ratio decreased from 0.27 to 0.2 with a growth in pore space volume of 20% to 40% in zirconia ceramics.

The fact that Poisson's ratio decreases with increasing pore space volume was previously noted in several publications. In [1,2] it was shown that for porous isotropic bodies, the values of Poisson's ratio depend on pore space volume, pore geometry and Poisson's constant values for a pore-free material state (μ_0). For materials with $\mu_0>0.2$ (including alumina and zirconia ceramics), it was theoretically predicted and experimentally proven that there is a decrease in the values of Poisson's ratio with the increase in pore space volume for ceramics with different pore geometry [1,2]. The decrease of Poisson's ratio with increasing pore space volume can be explained by nonlinear elasticity, demonstrated by porous ceramics under mechanical loading [4]. Furthermore, the local deformations caused by relative movements and deformations of their structural components play an essential role in the deformation of objects with a similar complicated internal structure, noticeably changing the elastic properties of metals [1].

SUMMARY

The analysis of strain-stress curves of porous alumina and zirconia ceramics showed that during deformation by compression and shearing, there was a transition from a brittle state typical for relatively dense ceramics, to a pseudo-plastic state with a high porosity level.

The values of the effective Young's modulus, effective shear modulus and Poisson's ratio decrease with increasing pore space volume of alumina and zirconia ceramics, which correlates with the appearance of multiple cracks in the course of the deformation of highly porous ceramics.

It was shown that during deformation by compression, the destruction process was controlled by shearing stresses, which leads to the formation of conical damages in the internal volume of object, the size and location of damages depending on the pore space volume.

ACKNOWLEDGEMENT

This work was done under partial financial support in the frame of Agreement No. 14.578.21.0035.

REFERENCES

1. K. K. Phani, J. Mater. Sci. **43**, 316–323 (2008).
2. M. L. Dunn and H. Ledbetter, J. Mater. Res. **10/11**, 2715–2722 (1995).
3. L. Gömze and L. Gömze, Mater. Sci. Forum **729**, 43 (2013).
4. S. N. Kulkov, V. I. Maslovskiy, S. P. Buyakova, and D. S. Nikitin, Tech. Phys. J. **72/3**, 38–42 (2002).
5. Yu. P. Stefanov, Fiz. Mezomekh. **13**(Spec. Iss.), 44–52 (2010).
6. N. L. Savchenko, T. Yu. Sablina, T. M. Poletika, A. S. Artish, and S. N. Kulkov, Powder Metall. **1–2**, 26–30 (1994).
7. R. V. Goldshtein, Mech. Adv. **2**, 3–17 (2003).